Free Radical Biology & Medicine 51 (2011) 503–515

Contents lists available at ScienceDirect

Free Radical Biology & Medicine

journal homepage: www.elsevier.com/locate/freeradbiomed

Original Contribution

Lipid hydroperoxide-induced and hemoglobin-enhanced oxidative damage to colon cancer cells

José Pedro F. Angeli, Camila Carrião M. Garcia, Fernanda Sena, Florencio P. Freitas, Sayuri Miyamoto, Marisa Helena G. Medeiros, Paolo Di Mascio *

Departamento de Bioquímica, Instituto de Química, Universidade de São Paulo, CEP 05508–000 São Paulo, SP, Brazil

ARTICLE INFO

Article history:
Received 16 October 2010
Revised 5 April 2011
Accepted 8 April 2011
Available online 14 April 2011

Keywords:
Lipid hydroperoxide
DNA damage
Oxidative stress
HPLC/ESI/MS-MS
DNA adducts
Free radicals

ABSTRACT

Epidemiological studies have indicated that Western diets are related to an increase in a series of malignancies. Among the compounds that are credited for this toxic effect are heme and lipid peroxides. We evaluated the effects of hemoglobin (Hb) and linoleic acid hydroperoxides (LAOOH) on a series of toxicological endpoints, such as cytotoxicity, redox status, lipid peroxidation, and DNA damage. We demonstrated that the preincubation of SW480 cells with Hb and its subsequent exposure to LAOOH (Hb + LAOOH) led to an increase in cell death, DCFH oxidation, malonaldehyde formation, and DNA fragmentation and that these effects were related to the peroxide group and the heme present in Hb. Furthermore, Hb and LAOOH alone exerted a toxic effect on the endpoints assayed only at concentrations higher than 100 μM. We were also able to show that SW480 cells presented a higher level of the modified DNA bases 8-oxo-7,8-dihydro-2′-deoxyguanosine and 1,N^2-etheno-2′-deoxyguanosine compared to the control. Furthermore, incubations with Hb led to an increase in intracellular iron levels, and this high level of iron correlated with DNA oxidation, as measured as EndoIII- and Fpg-sensitive sites. Thus, Hb from either red meat or bowel bleeding could act as an enhancer of fatty acid hydroperoxide genotoxicity, which contributes to the accumulation of DNA lesions in colon cancer cells.

The development of colorectal cancer (CRC) is a multistep process involving both somatic mutations and increased rates of cell proliferation. CRC most commonly occurs sporadically and is inherited in only 10% of the cases. Diet is the most important exogenous factor identified thus far in the etiology of this type of cancer [1]; support for this observation is given by studies showing that dietary modifications are able to reduce this cancer burden by up to 70% [2].

Colon cancer originates from the epithelial cells (colonocytes) that line the bowel. These cells are in direct contact with the contents of the lumen, making them one of the first cells to interact with exogenous compounds absorbed by the diet. Furthermore, epithelial cells of both the small intestine and the colon are among the most rapidly dividing cells in the body [3]. Rapid cell proliferation is a key factor in the development of cancer because damage to DNA may not be completely repaired before cell division occurs. In this case, DNA lesions can be converted to mutations. Supporting this assumption, Sjoblom et al. [4] analyzed 13,056 genes in colon and breast tumors and found a very high frequency of single-base substitutions, mainly of the GC/TA type. These data, although far from clarifying the exact source and mechanism of damage, tentatively point to the involvement of oxidatively generated DNA damage in such pathologies.

In recent years, research has focused on an attempt to identify compounds or interactions between compounds that could increase the genetic instability of colon cells and culminate in the appearance of malignancies, such as cancer [5]. Fat intake has been identified as one of the factors believed to play a major role in CRC. Indeed, fat intake has gained much attention in CRC because of the pioneering case–control study by Wynder et al. [6], which suggested that dietary fats might be involved in the pathogenesis of CRC. Subsequently, a large number of epidemiological comparisons conducted worldwide have shown that fats are associated with CRC [7–9]. Some of the discrepancies in the findings on this association may be attributable to the fact that dietary fats were mainly investigated according to their quantity (total fat), origin (animal or plant), or type (saturated, monounsaturated, or polyunsaturated) [10].

The evaluation of some epidemiological studies and experimental data have linked the dietary intake of ω-6 polyunsaturated fatty acids (PUFAs), such as linoleic acid (LA), to an increased risk for cancers of

Abbreviations: CRC, colorectal cancer; dGuo, 2′-deoxyguanosine; 8-oxodGuo, 8-oxo-7,8-dihydro-2′-deoxyguanosine; 1,N^2-εdGuo, 1,N^2-etheno-2′-deoxyguanosine; 1,N^2-propanodGuo, 1,N^2-propano-2′-deoxyguanosine; LAOOH, linoleic acid hydroperoxide; LAO•, linoleic acid alkoxyl radical; LAOO•, linoleic acid peroxyl radical; HNE, 4-hydroxynonenal; DDE, *trans,trans*-2,4-decadienal; MDA, malonaldehyde; $^1O_2$, singlet molecular oxygen; Hb, hemoglobin; HPLC, high-performance liquid chromatography; ECD, electrochemical detection; ESI/MS-MS, electrospray ionization tandem mass spectrometry; MRM, multiple reaction monitoring; H_2DCF-DA, 2′,7′-dichlorofluorescein diacetate; DCF, dichlorofluorescein; Fpg, formamidopyrimidine DNA glycosylase; EndoIII, endonuclease III.

* Corresponding author. Fax: +55 011 38155579.
E-mail address: pdmascio@iq.usp.br (P. Di Mascio).

0891-5849 © 2011 Elsevier Inc. Open access under the Elsevier OA license.
doi:10.1016/j.freeradbiomed.2011.04.015

the breast, colon, and possibly prostate, particularly when in combination with a low intake of ω-3 PUFAs or monounsaturated fatty acids [11]. Concern has been raised because LA (one of the most abundant fatty acids in the diet) has been linked to the development of cancer in animals [12,13], and some population comparisons have reported positive associations with per-capita use of polyunsaturated fatty acids [14,15]. Additionally, it was shown that people whose diet was supplemented with LA presented an increase in leukocyte levels of 8-oxo-7,8-dihydro-2′-deoxyguanosine (8-oxodGuo) [16]. An added concern is that polyunsaturated fats may be prone to oxidation and generate primarily lipid peroxides, which may play an overlooked role in carcinogenesis [17], because none of the above-mentioned studies analyzed the amount of peroxides in their LA preparations. Lipid peroxides are a major source of dietary oxidants, with mutagenic or carcinogenic potentials that are of nutritional and toxicological importance [18]. Because of their ability to generate oxyradicals, lipid peroxides are capable of initiating degenerative processes and promoting digestive system disorders, such as inflammation and cancer [19]. Likewise, lipid peroxidation has been linked to DNA damage in many physiopathological situations that include CRC [20]. The lipid peroxidation process generates aldehydes as secondary products, such as *trans*-4-hydroxy-2-nonenal (HNE), *trans,trans*-2,4-decadienal (DDE), malondialdehyde (MDA), and crotonaldehyde [21]. These compounds can lead to the formation of promutagenic oxidatively generated and exocyclic DNA adducts in human cells and may contribute to the onset of diet-related cancers [22–25].

In addition, it is estimated that humans with a normal diet consume an average of 84 g of fat daily, leading to an estimated intake of 1.5 mmol of lipid peroxides [26]. Nevertheless, based on other reports, it is conceivable to assume the following: the concentration of lipid hydroperoxides in the stomach may reach values up to 250 mM after ingestion of a high-fat meal, and because lipid hydroperoxides may be present with other nutrients, the concentrations may decrease to values of approximately 25 mM [27]. Studies by Kanazawa and Ashida [28,29] have demonstrated that trilinoleoylglycerol hydroperoxides are promptly deesterified, resulting in the free fatty acid linoleic acid hydroperoxide, and studies by Miyamoto et al. have also shown that 1-palmitoyl-2-linoleoylphosphatidylcholine hydroperoxide liberates the free fatty acid in the gastric mucosa [30]. Furthermore, it was shown that approximately 97% of peroxides are decomposed in the stomach and that, in animals, only a small fraction of LAOOH reached the intestine after the ingestion of a high amount of fat [29]. Thus, based on the above values (provided in [27]), one could expect maximum values of approximately 500 μM free fatty acids in the intestine. Human studies have shown that fecal water contains up to 1 mM fatty acids [31] and that a 20–30 μM fatty acid peroxide concentration could be easily achieved [32] in the colon of healthy volunteers. Moreover, it is expected that individuals consuming a high-fat diet could present an approximately 10-fold increased level of lipids and fatty acids and reach values near those previously described.

Another important link between nutrition and CRC has been proposed by studies of populations consuming high levels of red meat. Dietary epidemiological studies have indicated correlations between the consumption of red meat and/or processed meat and cancer of the colon and rectum [33]. Moreover, experimental data from humans have also shown that the intake of dietary heme is associated with an increase in the incidence of colon cancer [34]. Furthermore, the European Prospective Investigation into Cancer and Nutrition (EPIC) study group has reinforced a positive correlation between red meat/heme intake and the incidence of colorectal cancers [33]. It is often hypothesized that in addition to heme, the high fat content in red meat could also play a role in the onset of colorectal cancer [35].

The mechanism of cancer promotion by heme is not known, but some groups have proposed that it might be linked to oxidative stress [36,37]. It has been reported that heme, derived from hemoglobin, is able to induce DNA strand breaks in primary colon and colon cancer cells. The authors claimed that intracellular free iron is the primary genotoxicant because of the ability of the iron molecule to be released from the oxidized form of heme [38]. This is in agreement with several reports indicating that inorganic iron is genotoxic to colon cancer cells [39,40]. Furthermore, feeding rats with meat containing low, medium, or high heme concentrations led to an increase in heme in the intestinal lumen, reaching levels from 19 to 1097 μM [41], and the formation of preneoplastic lesions in this model strongly correlated with the heme/iron concentration found in the lumen. With respect to heme ingestion in humans, individuals present a concentration of approximately 400 μM iron in the gut lumen after a meal with high iron content [42]. Considering the fact that individuals consuming a Western-type diet present approximately 40% of their total iron intake as heme–iron [43], it could be expected that the concentrations of heme–iron may reach values higher than 100 μM.

Other studies have correlated heme-induced tumorigenesis with an increase in lipid peroxidation and proliferation. Indeed, this heme-induced tumor promotion was associated with increased lipid peroxidation and strong cytotoxic activity of fecal water in a cancerous mouse colonic epithelial cell line [44]. Moreover, the normalization of lipid peroxidation was able to inhibit heme-induced tumorigenesis, evidencing the importance of lipid peroxidation in the onset of the disease [45].

In this study, we offer an alternative explanation and a possible mechanism that links these two known etiologic agents, lipid peroxides and heme, with an increased colon cancer risk. In this context, we assume that an interplay between heme–iron and lipid peroxides promotes genomic instability and is one of the first steps in the onset of the carcinogenic process. Therefore, we used SW480 cells to examine the genotoxic effects of Hb and LAOOH, two compounds with pro-oxidant effects whose levels are increased in the colon of individuals consuming a high-fat/high-meat diet. Our results demonstrate that increased levels of heme–iron led to an increase in the DNA damage that is promoted by LAOOH at concentrations that are relevant to individuals consuming a high-fat and/or high-meat diet.

Materials and methods

Chemicals

Ethidium bromide (CAS: 1239-45-8), trypan blue (CAS: 72-57-1), hemoglobin (CAS: 9008-02-0), and ethylenediaminetetraacetic acid (EDTA; CAS: 150-43-6) were purchased from Sigma (St. Louis, MO, USA). Low-melting-point (LMP) agarose (CAS: 9012-36-6; Gibco) at 0.5% (w/v) and normal-melting-point agarose (CAS: 9012-36-6; Gibco) at 1.5% (w/v) were dissolved in Ca^{2+}- and Mg^{2+}-free phosphate-buffered saline (PBS).

All other chemicals, reagents, and buffers were analytical grade products from Sigma.

Synthesis of LAOOH

LAOOH was synthesized as described previously [46]. Briefly, 1 g of linoleic acid was dissolved in 50 ml of chloroform containing 0.2 mM methylene blue and irradiated with a tungsten lamp (500 W) for 5 h. The irradiation was conducted in an ice bath under a continuous flux of oxygen. LAOOH was separated by silica-gel column chromatography. The reaction products were placed on the column and separated by a discontinuous gradient of *n*-hexane:diethyl ether from 9:1 to 5:5 (v/v). The concentration of LAOOH was determined spectrophotometrically at 234 nm ($\varepsilon = 25 \times 10^3\ M^{-1}\ cm^{-1}$) because 60% of the hydroperoxides contained conjugated dienes, resulting in an approximately 50% conversion of LA to LAOOH. More details related to the synthesis and characterization of LAOOH can be found in the supplementary material (Supplementary Fig. 1). The corresponding LAOH was also synthesized as described previously [46].

Preparation of apo-Hb

The Hb solution was added to 40 ml of ice-cold HCl–acetone solution (2.5 ml of 2 M HCl in 1 L of acetone). The mixture was vigorously stirred for 30 min on ice and centrifuged at 13,000*g* for 10 min. The supernatant was discarded, and the pellet was washed three times with HCl–acetone. The pellet was redissolved in water and then dialyzed extensively against water. After the dialysis, the protein suspension was centrifuged at 6000*g* for 5 min; the suspension was then lyophilized and stored at −20 °C.

Cell culture

The human colon adenocarcinoma cell line (SW480 cells) was a kind gift from Prof. Dr. Mary Cleide Sogayar (Instituto de Quimica, Universidade de São Paulo). The SW480 cells were maintained in Dulbecco's modified Eagle medium supplemented with 15% FBS and 1% penicillin–streptomycin; under these culture conditions, the doubling time was approximately 24 h. For all of the experiments, cells from 15th and 25th passages were used.

Cell treatments

For the genotoxicity assays, the SW480 cells were first grown for a complete cell cycle (24 h) and then washed twice with PBS–diethylenetriaminepentaacetic acid (DTPA; 0.1 mM). Next, the test compounds were added to the PBS–DTPA (treated with Chelex) for 1 h and assayed for the various toxicological endpoints. For experiments involving pretreatment with Hb, cells were grown for 24 h before being washed and then treated with the indicated concentration of Hb for various durations in the cell culture medium. The cells were then washed five times with PBS–DTPA and incubated with LAOOH for 1 h in PBS–DTPA and subsequently assayed.

Cytotoxicity (3-(4,5-dimethylthiazol-2-yl)-2,5-diphenyltetrazolium bromide (MTT) assay)

The influence of LAOOH and the combination of Hb and LAOOH were assayed by the MTT assay in 96-well microtiter plates. Briefly, after treatment, the cells were washed and incubated for various periods (6, 24, or 48 h). After the incubation period, the medium was carefully collected, and the cells were incubated with 250 μg/ml MTT for 3 h. The cells were then washed and resuspended in dimethyl sulfoxide (DMSO), and the absorbance at 540 nm was measured. The results are expressed as the percentage of viable cells in relation to the control.

Production of reactive oxygen species as determined by the dichlorofluorescein assay

Intracellular reactive oxygen species (ROS) were estimated using the fluorescent probe 2′,7′-dichlorofluorescein diacetate (H_2DCF-DA) [47]. H_2DCF-DA diffuses through the cell membrane and is enzymatically hydrolyzed by intracellular esterases to form nonfluorescent H_2DCF, which is oxidized to fluorescent dichlorofluorescein (DCF) by ROS. Thus, the fluorescence intensity of DCF is proportional to the production of intracellular ROS. After the described treatments (see Cell treatments), the fluorescence was measured by fluorimetry (excitation at 485 nm, emission at 538 nm). The results are expressed in relation to the values from control cells.

Malonaldehyde quantification

MDA was measured as previously described by Tatum et al. [48]. After treatment, 7 ml of a 0.4% (w/v) solution of 2-thiobarbituric acid (TBA) in 0.2 N HCl:H_2O (2:1) and 1 ml of a 0.2% (w/v) solution of butylhydroxytoluene in 95% ethanol were added to the cell samples, and the mixture was heated to 90 °C for 45 min, cooled on ice, and extracted with isobutanol. The isobutanolic phase was injected through a Shimadzu autoinjector, Model SIL-10AD/VP (Shimadzu, Kyoto, Japan), into a Shimadzu HPLC system, which consisted of two pumps (LC-6AD) connected to a Lichrosorb 10 RP-18 (Phenomenex, Torrance, CA, USA) reversed-phase column (250 × 4.6-mm i.d.) with a particle size of 10 μm. The flow rate of the isocratic eluent (25 mM potassium phosphate buffer, pH 7, in 40% methanol) was 1 ml/min. An RF-10A/XL fluorescence detector was set at an excitation wavelength of 515 nm and an emission wavelength of 550 nm. The data were processed using the Shimadzu Class-VP 5.03 software. The malonaldehyde–bis-diethylacetal adduct with TBA was used for the calibration of the fluorescence data. The data were expressed as micromoles of MDA normalized to the protein content, which was determined by the Bradford method.

Estimation of peroxide content (FOX assay)

Extracellular LAOOH was determined according to Dringen and Hamprecht [49]. This assay can be used to determine compounds capable of oxidizing Fe^{2+}. Briefly, 10 μl of the LAOOH-containing incubation buffer, collected after gentle swirling of the dish at the time points indicated, was added to 190 μl of 25 mM H_2SO_4 in the well of a microtiter plate. Forty-five minutes after the further addition of 200 μl of reaction mixture (0.5 mM $(NH_4)_2Fe(SO_4)_2$, 200 mM sorbitol, and 200 μM xylenol orange in 25 mM H_2SO_4), the extinction coefficient was determined using a microtiter-plate reader (at 540 nm; Tecan, Männedorf, Switzerland). The intracellular peroxide content was determined according to the protocol described by Gay and Gebicki [50]. Briefly, the lipid phase was assayed in 1:2 acetic acid:methanol (G–PCA–FOX), with water replacing the methanol for the aqueous samples (M–PCA–FOX).

Single-cell gel electrophoresis (comet assay)

The single-cell gel electrophoresis assay was carried out according to the protocol of Uhl et al. [51]. Approximately 5×10^4 cells were mixed with LMP agarose and then transferred to agarose-coated slides, covered with a coverslip, and cooled at 4 °C for 20 min. After removal of the coverslips, the slides were immersed in fresh lysis solution composed of 89 ml of lysis stock solution (2.5 M NaCl, 100 mM EDTA, 10.0 mM Tris, pH 10, adjusted with solid NaOH, and 890 ml distilled water), 1.0 ml of Triton X-100 (Merck), and 10 ml of DMSO. Cells were lysed for 2 h at 4 °C in the dark, and the slides were then transferred to an alkaline solution (300 mM NaOH and 1 mM EDTA, pH 13.0, prepared from a stock solution of 10 M NaOH and 200 mM EDTA) at 4 °C for 40 min to denature the DNA. Electrophoresis was performed at 25 V and 300 mA (25 V/cm) for 20 min. The slides were then neutralized with three washes, each for 5 min, of pH 7.5 buffer (0.4 M Tris–HCl), air dried, fixed in absolute ethanol for 10 min, and stored for later scoring. In addition, a small aliquot of the cells was assayed in parallel for cytotoxicity by the trypan blue method to avoid any interference with the assay. The slides were stained by adding 100 μl of ethidium bromide (20 μg/ml); a coverslip was placed over the cells, which were then evaluated with a fluorescence microscope (Nikon) at 20×, using a 420–490 nm excitation filter and a 520 nm barrier filter. A total of 100 cells per treatment were inspected with the aid of the software KOMET 6.0 (Andor). DNA damage is expressed as the Olive tail moment.

Modified comet assay

The comet assay was modified by the addition of formamidopyrimidine glycosylase (Fpg) and endonuclease III (EndoIII), which recognize the oxidized forms of purines and pyrimidines, respectively,

and convert them to strand breaks. After lysis, slides for the measurement of oxidized bases were washed three times in enzyme buffer (0.1 M KCl, 0.5 mM Na_2EDTA, 40 mM *N*-2-hydroxyethylpiperazine-*N*-2-ethanesulfonic acid, and 0.2 mg/ml bovine serum albumin, pH 8.0) and then incubated for 30 min at 37 °C with the appropriate enzyme (EndoIII from *Escherichia coli* and Fpg from *E. coli;* Sigma–Aldrich) or enzyme buffer alone (control). The subsequent steps were identical to the standard version of the assay (see the previous section).

DNA adduct determination

DNA isolation

DNA was isolated by the chaotropic NaI method, as previously described [52]. Briefly, cellular pellets (3×10^8 cells) were homogenized in 10 ml of a lysis solution (320 mM sucrose, 5 mM $MgCl_2$, 10 mM Tris–HCl, 0.1 mM desferroxamine, and 1% (v/v) Triton X-100, pH 7.5). After centrifugation at 1500*g* for 10 min, the pellets were resuspended in another 10 ml of the lysis solution and centrifuged once more at 1500*g* for 10 min. The pellets were then suspended in 6 ml of 10 mM Tris–HCl buffer, pH 8.0, containing 5 mM EDTA, 0.15 mM desferroxamine, and 350 μl of 10% SDS. The enzymes RNase A (30 μl, 10 mg/ml) and RNase T1 (4 μl, 20 U/μl) in 10 mM Tris–HCl buffer, pH 7.4, containing 1 mM EDTA and 2.5 mM desferroxamine, were added, and the reaction mixture was incubated at 37 °C. After 1 h, 300 μl of proteinase K (20 mg/ml) was added, followed by an additional incubation at 37 °C for 1 h. After centrifugation at 5000*g* for 15 min, the liquid phase was collected and 4 ml of a solution containing 7.6 M NaI, 40 mM Tris–HCl (pH 8), 20 mM EDTA, and 0.3 mM desferroxamine was added, followed by the addition of 8 ml of isopropanol. The contents were mixed by inversion until a whitish precipitate appeared. The precipitate was collected by centrifugation at 5000*g* for 15 min and washed with 5 ml of isopropanol 60% (5000*g*, 15 min), followed by 5 ml of ethanol 70% (5000*g*, 15 min). The DNA pellet was solubilized in 500 μl of desferroxamine (0.1 mM), and the DNA concentration was measured spectrophotometrically at 260 nm.

Enzymatic hydrolysis of DNA

Four microliters of 1 M sodium acetate buffer (pH 5) and 100 fmol of [$^{15}N_5$]1,N^2-etheno-2'-deoxyguanosine ([$^{15}N_5$]-1,N^2-εdGuo) and [$^{15}N_5$]1,N_2-propano-2'-deoxyguanosine ([$^{15}N_5$]-1,N^2-propanodGuo) were added to an aliquot of 0.1 mM desferroxamine solution containing 200 μg of DNA, followed by digestion with 2 units of nuclease P1 at 37 °C for 30 min. Twelve microliters of 1 M Tris–HCl buffer (pH 7.4), 12 μl of phosphatase buffer, and 6 units of alkaline phosphatase were then added for an additional 1-h incubation at 37 °C. The final volume of the solution was adjusted to 200 μl with water. The enzymes were precipitated by the addition of 1 volume of chloroform and, after centrifugation at 1000*g* for 5 min, the resulting aqueous layer was subjected to HPLC/ESI/MS-MS analysis (100 μl of the DNA solution/injection). The amounts of the reagents and labeled internal standard were proportionally adjusted for hydrolysis and the analysis of other DNA quantities.

Analysis of 8-oxodGuo using HPLC/EC

Samples (100 μg) of digested DNA were injected into the HPLC/EC system, which consisted of a Shimadzu Model LC-10 AD pump (Shimadzu) connected to a Luna C18 analytical column (250×4.6-mm i.d.) with a particle size of 5 μm (Phenomenex) and maintained at 16 °C by a CTO-10AS VP column oven (Shimadzu). The isocratic eluent was 25 mM potassium phosphate buffer, pH 5.5, and 8% methanol at a flow rate of 1 ml/min. Colorimetric detection was performed using a Coulochem II detector (ESA, Chelmsford, MA, USA), and spectrophotometric detection was performed using a Shimadzu SPD-10A (Shimadzu). The potential of the electrode was set at +280 mV for the detection of 8-oxodGuo. A Shimadzu SPD-10AV/VP UV detector set at 254 nm simultaneously monitored the elution of unmodified nucleosides. The Shimadzu Class-LC10 1.6 software was used to calculate the peak areas. The molar ratio of 8-oxodGuo to 2′-deoxyguanosine (dGuo) in each DNA sample was determined based on the coulmetric detection at 280 mV for 8-oxodGuo and absorbance at 254 nm for dGuo in each injection.

Synthesis of 1,N^2-εdGuo and [$^{15}N_5$]1,N^2-εdGuo standards

The 1,N^2-εdGuo standard was obtained by the reaction of 40 mM dGuo with 2 M chloroacetaldehyde, as described previously. The [$^{15}N_5$]1,N^2-εdGuo standard was obtained by the reaction of [$^{15}N_5$] dGuo with 2 M chloroacetaldehyde and subsequently purified by HPLC, as described by Loureiro et al. [53].

Synthesis of 1,N^2-propano-2'-deoxyguanosine (1,N^2-propanodGuo) and [$^{15}N_5$]1,N^2-propanodGuo standards

dGuo (25 μmol) was dissolved in 2 ml of 100 mM phosphate buffer, pH 8, 1 mM acetaldehyde, and 0.05 mM lysine. The mixture was shaken at 500 rpm at 37 °C for 24 h. The products were subsequently purified by HPLC, as described by Garcia et al. [54].

Analysis of 1,N^2-εdGuo and 1,N^2-propanodGuo by HPLC/ESI/MS-MS

Online HPLC/ESI/MS-MS analyses in the positive mode were carried out using an API-4000 QTRAP mass spectrometer (Applied Biosystems, Foster City, CA, USA). The 1,N^2-εdGuo and 1,N^2-propanodGuo adducts in the DNA samples were detected by multiple reaction monitoring (MRM). An Agilent HPLC system (Kyoto, Japan) that consisted of an autosampler (1200 High Performance), a column oven (1200 G1216B) set to 18 °C, an automated switching valve, a 1200 Binary Pump SL, a 1200 Isocratic Pump SL, and a UV detector (1200 DAD G1315C) was used for sample injection and cleanup of the analytical column (Luna C18 250×4.6-mm i.d., with a particle size of 5 μm) (Phenomenex). The adduct was eluted from this column with a gradient of formic acid (0.1% in water) and acetonitrile (from 0 to 10 min, 10% acetonitrile and 0.65 ml/min to 40% acetonitrile and 0.2 ml/min; from 10 to 16 min, 40 to 30% acetonitrile and 0.2 ml/min; from 16 to 20 min, 30 to 60% acetonitrile and 0.2 ml/min; from 20 to 21 min, 60 to 40% acetonitrile and 0.2 ml/min; from 21 to 22 min, 40 to 90% acetonitrile and 0.2 to 0.65 ml/min; from 22 to 26 min, 90% acetonitrile and 0.65 ml/min; from 26 to 27 min, 90 to 10% acetonitrile and 0.65 ml/min; and from 27 to 32 min, 10% acetonitrile and 0.65 ml/min).

An isocratic pump was used to simultaneously load a second column (Eclipse XDB-C18 150×4.6-mm i.d., with a particle size of 5 μm) (Agilent) with 0.2 ml/min of a (60:40) solution of water: acetonitrile with 0.1% formic acid, and a constant flow of the mobile phase to the mass spectrometer was maintained during the analysis. The position of the switching valve was changed twice: (1) at 13 min to allow the first column eluent to enter the second column and (2) at 25 min to wash the first column while the adduct was eluted through a second column and then transferred to the mass spectrometer. The total time spent on this analysis was 32 min. The automated switching valve directs unmodified nucleotides, after elution through column 1 and UV detection, to the waste (cleaning time 13 min), and this prevents loss of the mass spectrometer sensitivity.

The DNA hydrolysates, containing 100 fmol of the [$^{15}N_5$]1,N^2-εdGuo and [$^{15}N_5$]1,N^2-propanodGuo internal standards, were injected into the system described above. The *m/z* 292→176 (1,N^2-εdGuo), 297→181 ([$^{15}N_5$]1,N^2-εdGuo) $[M+H]^+$ and *m/z* 338→222 (1,N^2-propanodGuo), 343→227 ([$^{15}N_5$]1,N^2-propanodGuo) $[M+H]^+$ ions were monitored with a 200-ms dwell time.

All of the parameters of the mass spectrometer were adjusted for the acquisition of the best $[M+H]^+/[M+H-2\text{-D-}erythro\text{-pentose}]^+$ transition. The curtain gas was adjusted to 25 psi, the source temperature was held at 450 °C, the nebulizer and auxiliary gas were kept at 60 psi, the turbo ion spray voltage was set to 5500 V, the collision gas was set on high, the interface heater was held at 100 °C, and the entrance potential was at 10 V. The 338 → 222 and 343 → 227

transitions were selected at a 19-V collision energy setting, a 20-V collision cell exit, and a 51-V declustering potential. For the 292 → 176 and 297 → 181 transitions, the parameters were 17, 16, and 41 V, respectively (Supplementary Fig. 2). The data were processed using Analyst 1.4.2.

Quantification of intracellular iron content

The intracellular iron content was determined as described previously by Glei et al. [37]. Briefly, cells were exposed to 50 μM Hb for various time periods (0–540 min), washed, lysed by a freeze–thaw method, and quantified by inductively coupled argon plasma-emission spectrometry.

Results

Cytotoxicity

To evaluate the cytotoxicity of LAOOH and Hb, we employed an MTT assay. The LAOOH showed a dose–response effect and was cytotoxic after 24 h of incubation and at concentrations higher than 100 μM (Figs. 1A, C, and E). Furthermore, the preincubation of cells with Hb (50 μM) for 60 min potentiated the cytotoxicity of LAOOH. Control experiments with LA, LAOH, and apo-Hb were also performed. The results demonstrate that the pretreatment of cells with Hb potentiated LAOOH toxicity but not LAOH toxicity; furthermore, preincubation with apo-Hb presented no potentiation in the toxic effect of LAOOH (Figs. 1B, D, and F).

Oxidative stress parameters: MDA quantification and DCFH oxidation

The oxidative stress of cells exposed to LAOOH with or without pretreatment with Hb was measured by MDA formation and DCFH oxidation (Figs. 2A and C, respectively) and presented a dose-dependent response. Exposure of cells to LAOOH for 1 h induced DCFH oxidation and lipid peroxidation, as measured by MDA formation, only at higher concentrations (50 μM). Furthermore, the preincubation of cells with Hb (50 μM) for 1 h potentiated the DCFH oxidation and MDA formation that was induced by LAOOH in a dose-dependent manner. We further explored the role of the peroxide group and heme in the MDA and DCFH oxidation by pretreating also with Hb or apo-Hb and then challenging with solvent, LAOH, or LAOOH. The results of the assay for MDA formation and DCFH oxidation (Figs. 2B and D, respectively) show that the effect was observed only for LAOOH and cells pretreated with Hb.

Extracellular and intracellular peroxide measurements

The peroxide content of the extracellular media of cells exposed to LAOOH without or with pretreatment with apo-Hb and Hb was measured by the FOX assay. The results from this experiment are presented in Fig. 3A; no difference in the extracellular peroxide consumption was observed. Furthermore, we also assayed the intracellular peroxide content using a modified version of the FOX assay; protocols with and without the addition of apo-Hb and Hb were used, with the subsequent addition of ethanol, LAOH, or LAOOH (Fig. 3B). Only LAOOH was able to induce the accumulation of

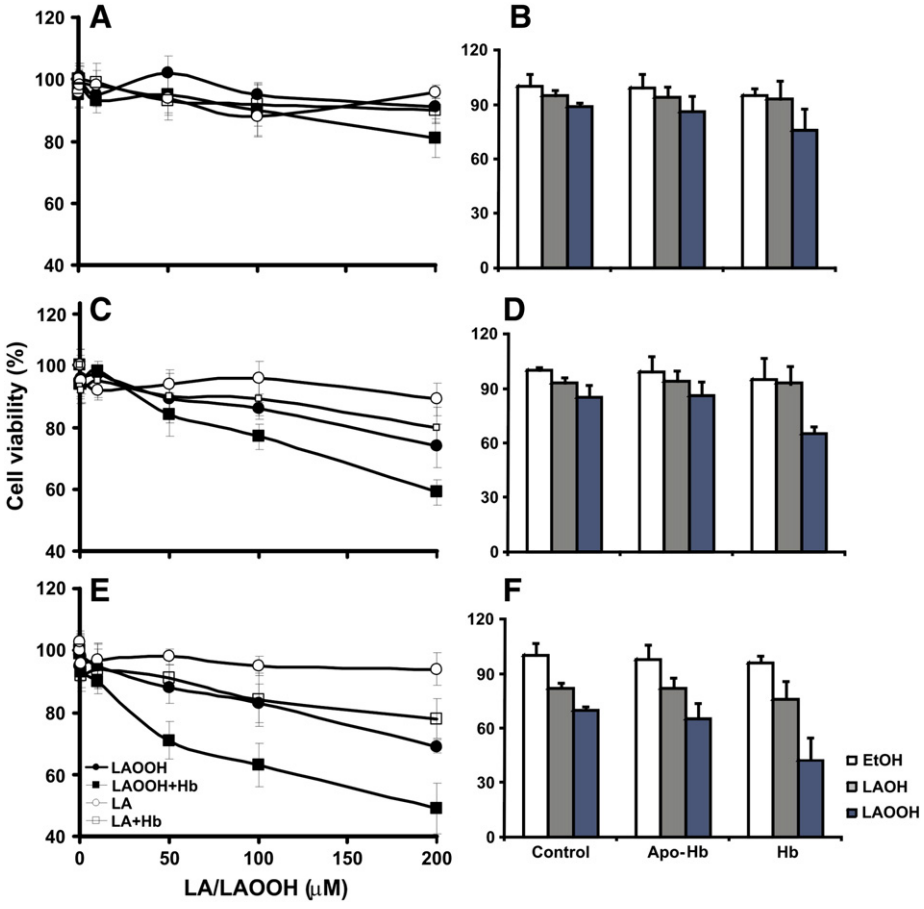

Fig. 1. Cell viability. For all of the experiments, cells were pretreated with or without 50 μM Hb for 1 h. Cells were then challenged with several concentrations of LAOOH or LA (0–200 μM) for (A) 6, (C) 24, or (E) 48 h. After the incubation period, cell viability was assessed through the MTT assay. Furthermore, the effects of peroxide and heme were assayed by treating cells for 1 h with 50 μM apo-Hb or Hb and subsequently exposing them to 200 μM LAOOH or LAOH for (B) 6, (D) 24, or (F) 48 h. Cell viability was then assessed through the MTT assay. For each experimental point, three independent experiments were carried out. Bars represent means ± standard deviations.

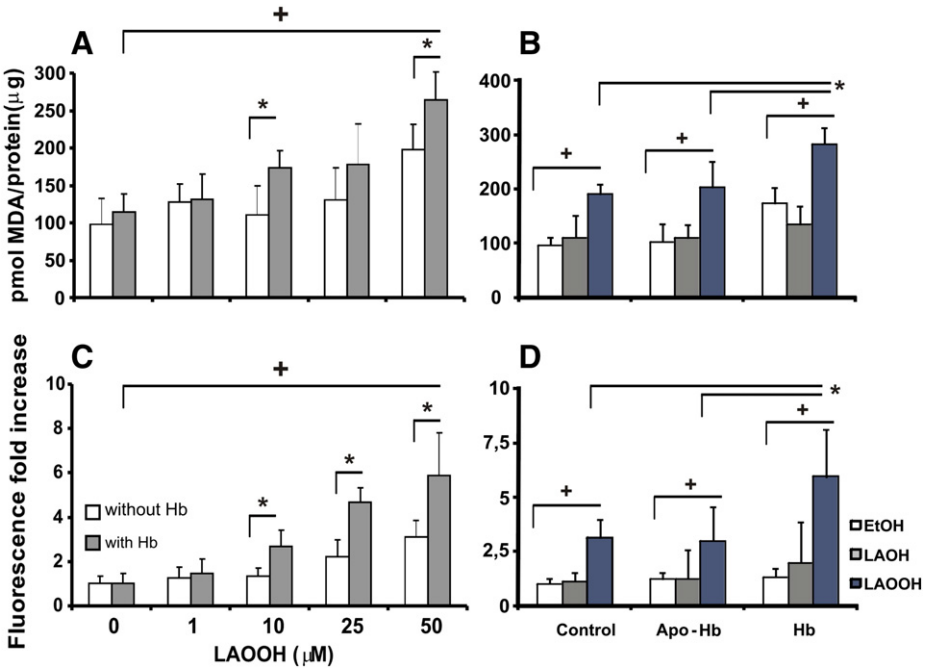

Fig. 2. Oxidative-stress parameters. For all of the experiments, cells were pretreated with or without 50 μM Hb for 1 h. Cells were then challenged with several concentrations of LAOOH (0–50 μM) and subsequently assayed for (A) MDA formation and (C) DCFH oxidation. Furthermore, the effects of peroxide and heme were assayed by treating the cells for 1 h with 50 μM apo-Hb or Hb and subsequently exposing them to 50 μM LAOOH or LAOH for 1 h and assaying for (B) MDA formation and (D) DCFH oxidation. Per experimental point, three independent experiments were carried out. Bars represent means ± standard deviations. Statistical significance was evaluated by two-way ANOVA. $^{*}p<0.05$, statistically different from cells that were not pretreated with Hb; $+p<0.05$, statistically different from cells not exposed to LAOOH.

peroxides, and this accumulation was found mainly in the organic fraction. In agreement with the previous results that Hb pretreatment was able to potentiate peroxide damage, a slight increase in peroxide accumulation in the cells exposed to apo-Hb was also observed.

Genotoxicity of Hb and LAOOH: alkaline and modified comet assay with Fpg and EndoIII

The results of the genotoxic effects of Hb and LAOOH are presented in Figs. 4A and C, respectively. Hb exhibited genotoxic effects only at concentrations up to 250 μM, whereas LAOOH did not present any visible effect, as measured by the standard version of the comet assay. However, the use of the modified version of the comet assay, with the addition of specific endonucleases, demonstrated that both compounds were able to induce DNA oxidation that was detected by measuring Fpg- and EndoIII-sensitive sites. Hb and LAOOH were effective at inducing DNA oxidation at concentrations of 100 and 50 μM, respectively (Figs. 4B and D, respectively). Moreover, the pretreatment of cells with Hb (50 μM) for 1 h markedly increased their sensitivity to the DNA damage induced by LAOOH. Fig. 4E depicts the results of the genotoxicity assayed by the standard version of the comet assay. The pretreatment of cells increased the number of LAOOH-induced strand breaks, and incubation with Fpg and EndoIII increased the levels of fragmentation under this condition (Fig. 4F) and also led to an increase in the number of EndoIII-sensitive sites. Figs. 4G through I present representative comet micrographs of cells exposed to solvent, 50 μM Hb, or 50 μM Hb plus the addition of 50 μM LAOOH, respectively. Moreover, to characterize the effects of the peroxide and heme group, cells were treated with apo-Hb or Hb and challenged with ethanol (EtOH), LAOH, and LAOOH; as was demonstrated for previously assayed parameters, the DNA damage effect, in both the standard and the enzyme-based assays, was

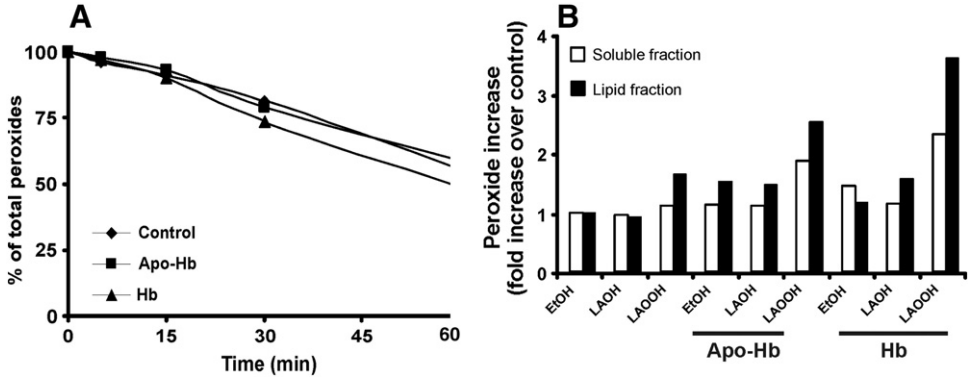

Fig. 3. Peroxide estimation in extracellular and intracellular compartments. (A) Clearance of LAOOH from the incubation buffer of SW480 cells. After a 30-min preincubation of the cells in incubation buffer containing 50 μM Hb and apo-HB, the cells were extensively washed and incubated in 50 μM LAOOH. The content of cellular protein was determined for each individual condition and used to normalize the results. (B) Intracellular peroxide content. Cells were treated as above and subsequently assayed by the M–PCA–FOX method (soluble fraction) or the G–PCA–FOX (lipid fraction). The data points were derived from duplicate measurements.

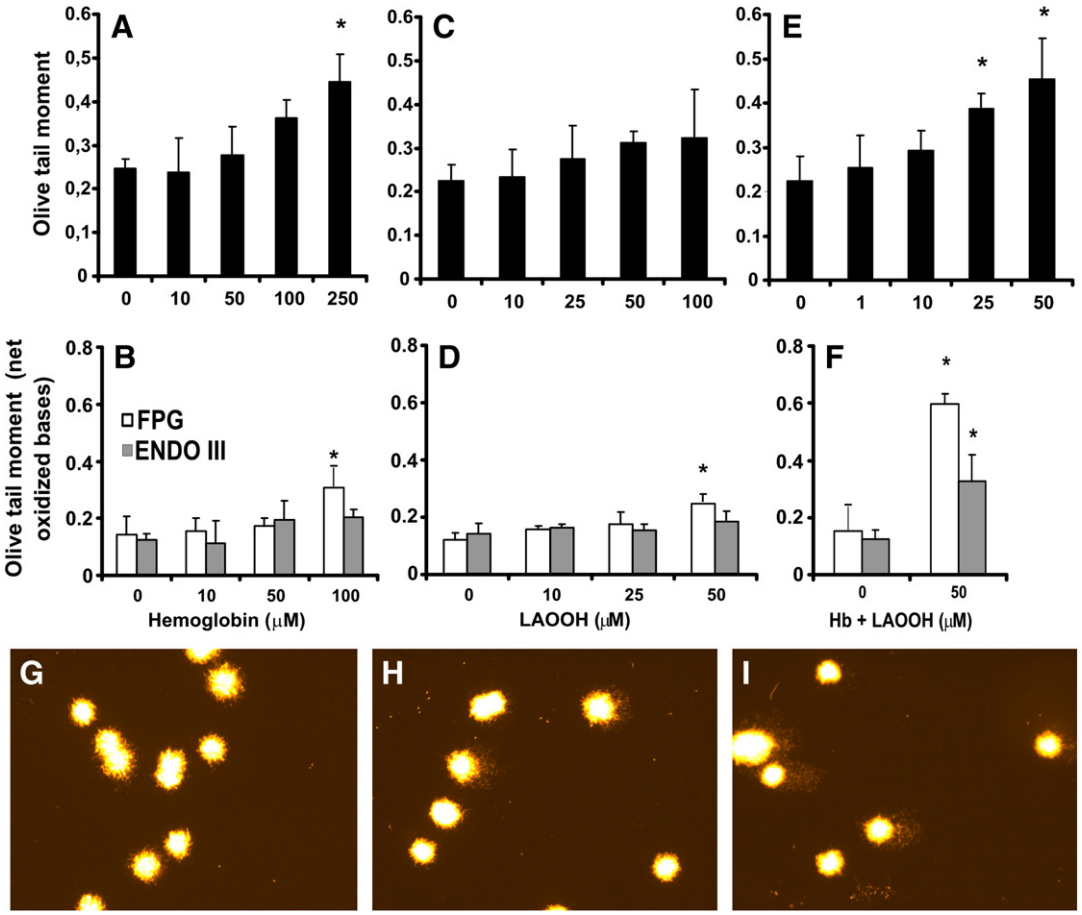

Fig. 4. DNA damage as measured by the comet assay. For the standard comet assay experiments, cells were treated with several concentrations of (A) Hb (0–250 μM) and (C) LAOOH (0–100 μM); (E) regarding pretreatment, cells were treated for 1 h with 50 μM Hb and, subsequently, treated with several concentrations of LAOOH (0–50 μM). Cells were then assayed for DNA damage. For the enzyme-based assay, cells were treated as above, (B) Hb (0–100 μM), (D) LAOOH (0–50 μM), and (F) pretreatment. After exposure to the test compounds for 60 min, the formation of comets was analyzed by use of a computer-aided analysis system. Per experimental point, three independent experiments were carried out, and, from each culture, 50 cells were analyzed for comet formation. Bars represent means ± standard deviations. The results are presented as Olive tail moment, and the enzyme-based assay is expressed as net oxidized bases. Statistical significance was evaluated by two-way ANOVA (*$p<0.05$). (G through I) Representative comet micrographs of cells exposed to solvent, 50 μM Hb, or 50 μM Hb plus the addition of 50 μM LAOOH, respectively.

dependent on the peroxide and the heme group (Fig. 5A). Figs. 5B through D present representative comet micrographs of cells pretreated with 50 μM Hb for 60 min and subsequently challenged with EtOH, 50 μM LAOH, and 50 μM LAOOH, respectively.

Quantification of specific DNA lesions: 8-oxodGuo, 1,N^2-εdGuo, and 1,N^2-propanodGuo

For an evaluation of DNA adducts, cells were incubated with either PBS–DTPA–0.05% methanol (control cells) or PBS–DTPA containing each of the following compounds at 50 μM: Hb, LAOOH, or LAOOH with Hb pretreatment. Figs. 6A–C depict the quantification of 8-oxodGuo in SW480 cells. The UV spectrum (λ = 265 nm) of DNA samples showing thymine (Thd), cytosine, dGuo, and adenine is presented in Fig. 6A. Fig. 6B depicts the corresponding peak of 8-oxodGuo in the electrochemical chromatogram. The amount of 8-oxodGuo in the Hb + LAOOH samples increased approximately threefold, compared to the control cells. The results are expressed as 8-oxodGuo/10^6 dGuo and are presented in Fig. 5C.

Regarding lipid peroxidation-derived DNA adducts, we developed an HPLC program that allowed the adequate separation of the adducts from Thd, the last eluted nucleoside, as shown in Supplementary Fig. 2. The method also allows for the simultaneous quantification of dGuo from hydrolyzed DNA samples through an absorbance measurement (λ = 260 nm) in the UV detector (Supplementary Fig. 2E). An automated switching valve (Supplementary Fig. 2F) was programmed to change its position in the interval between the end of elution of the last-eluted DNA base and the beginning of elution of the first-eluted DNA adduct (1,N^2-εdGuo). A representative MRM chromatogram of the 1,N^2-εdGuo, 1,N^2-propanodGuo analysis of cellular DNA is presented in Supplementary Figs. 2A and C. The use of the stable isotopic internal standards, [$^{15}N_5$]1,N^2-εdGuo and [$^{15}N_5$]1,N^2-propanodGuo, 5 units of mass larger than the native adducts, ensured the accurate quantification of the adducts (Supplementary Figs. 2B and 2D). The stable isotopic internal standards (100 fmol) were added to the DNA samples before the enzymatic hydrolysis. The *m/z* transition chosen for the MRM-detection experiments is a predominant fragmentation that results in a loss of 116 mass units, which is the [M+H − 2-D-*erythro*-pentose]$^+$ ion of the adducts. The representative ion chromatograms obtained by MRM detection using the respective *m/z* transitions from 292 to 176 (1,N^2-εdGuo), from 297 to 181 ([$^{15}N_5$]1,N^2-εdGuo), from 338 to 222 (1,N^2-propanodGuo), and from 343 to 227 ([$^{15}N_5$]1,N^2-propanodGuo), which correspond to 500 amol of unlabeled adducts and 33 fmol of stable isotopic internal standards, are shown in Supplementary Figs. 2A–2D. The results of the quantification of the exocyclic DNA adducts, 1,N^2-εdGuo and 1,N^2-propanodGuo, are presented in Figs. 7A and 7B, respectively. 1,N^2-εdGuo (Fig. 7A) was observed in almost 2.5-fold excess in cells treated with LAOOH that had been preincubated with Hb. 1,N^2-propanodGuo (Fig. 7B) levels were slightly higher but were not

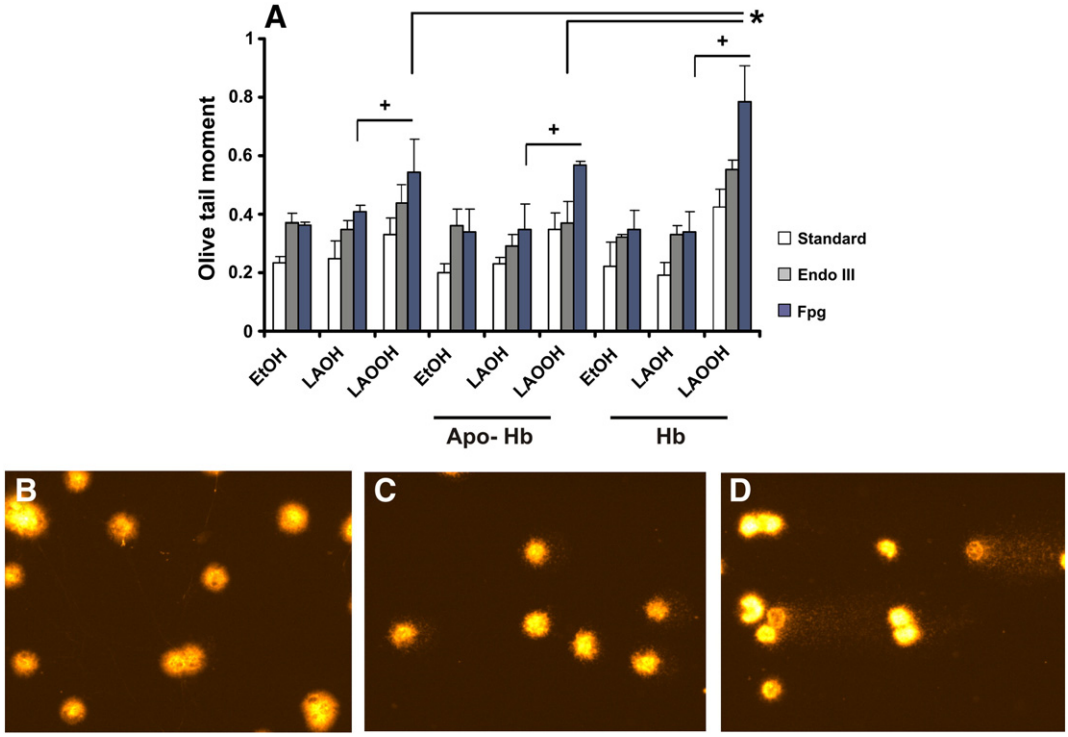

Fig. 5. Effects of peroxide and heme on DNA damage, as measured by the comet assay. (A) The effects of peroxide and heme were assayed by treating cells for 1 h with 50 μM apo-Hb or Hb and, subsequently, challenging them with 50 μM LAOOH or LAOH for 1 h. After exposure to the test compounds, the formation of comets was analyzed by use of a computer-aided analysis system. Per experimental point, three independent experiments were carried out, and, from each culture, 50 cells were analyzed for comet formation. Bars represent means ± standard deviations. Results are presented as Olive tail moment. Statistical significance was evaluated by two-way ANOVA. $^{*}p<0.05$, statistically different from Hb; $+p<0.05$, statistically different from EtOH and LAOH. (B through D) Representative comet micrographs of cells pretreated with 50 μM Hb for 60 min and then challenged with EtOH, 50 μM LAOH, and 50 μM LAOOH, respectively.

statistically significant, as neither Hb nor LAOOH alone was able to induce such lesions. Furthermore, the apo-Hb and LAOH did not alter the formation of 1,N^2-εdGuo and 1,N^2-propanodGuo.

Relationship between iron content and DNA oxidation

The intracellular iron content in cells treated with Hb is presented in Fig. 8A. The iron content increased in a time-dependent manner in cells incubated with 50 μM Hb but reached a plateau after ~120 min.

We also explored the role of iron uptake in DNA oxidation measured by the Fpg- and EndoIII-modified versions of the comet assay. These results are shown in Fig. 8B. There was an increase in damage levels upon treatment with 50 μM LAOOH in cells exposed for various incubation times to 50 μM Hb, up to ~90 min. A prolonged time of Hb incubation led to protection against the damage induced by LAOOH. Figs. 8C and D present the correlation between the iron content and the frequency of EndoIII- or Fpg-sensitive sites, respectively. Only the first stages of incubation are plotted in these graphs. In the earliest stages of incubation with Hb, there is a strong correlation between iron content and oxidized bases ($r^2=0.88$ for Fpg sites, Fig. 8D, and $r^2=0.9$ for EndoIII, Fig. 8C). Figs. 8E through H present representative comet micrographs of cells pretreated with 50 μM Hb for 0, 15, 60, and 240 min, respectively, and subsequently challenged with 50 μM LAOOH.

Discussion

Colorectal cancer is a common and often lethal disease in Westernized societies. The Western diet includes an excess of fat and red meat but is low in fiber and calcium [55]. We have hypothesized that interactions between pro-oxidant compounds can lead to an enhancement of toxicological parameters. Therefore, we assessed the effects of dietary-relevant concentrations of both compounds on cytotoxicity, oxidative stress, and genotoxicity in SW480 colon cancer cells, and we demonstrated that heme–iron is able to enhance LAOOH toxicity.

According to the results of the comet assay in our study, Hb alone presented genotoxicity at concentrations higher than 250 μM. These data are in agreement with the previous work of Glei et al. [37], who showed that Hb could induce DNA damage in colon cells in concentrations ranging from 250 to 500 μM. The addition of Fpg showed that lower concentrations (100 μM) of Hb induced Fpg-sensitive sites, as measured by strand breaks. The study of Glei et al. [37], evaluating the effects of hemoglobin, hemin, and myoglobin on induced DNA damage, showed that these compounds were able to induce DNA damage that was correlated with increased iron–heme concentrations. This iron–heme could, in turn, be degraded, releasing free iron that could then catalyze the decomposition of peroxides. Nevertheless, the production of secondary oxidants could not be discounted because the autoxidation of hemoglobin–heme could generate $O_2^{\bullet-}$ [56], which, in turn, could be dismutated to hydrogen peroxide and consequently react with free iron or heme inside the cells, leading to the formation of species reactive enough to damage DNA. Additional experiments corroborating this hypothesis are presented in the supplementary material (Supplementary Fig. 3).

Regarding LAOOH alone, no genotoxicity, as determined by the standard versions of the comet assay, was observed. Nevertheless, the addition of Fpg led to an increase in strand breaks after incubation with 100 μM LAOOH. This genotoxic effect of LAOOH is consistent with the findings of Kaneko et al. [57], who studied the formation of 8-oxodGuo in cells preincubated with Fe–NTA and exposed to LAOOH. In our study, we demonstrated that 8-oxodGuo was generated in cells preincubated with Hb and then exposed to LAOOH. The formation of 8-oxodGuo and the increase in Fpg-sensitive sites are of great

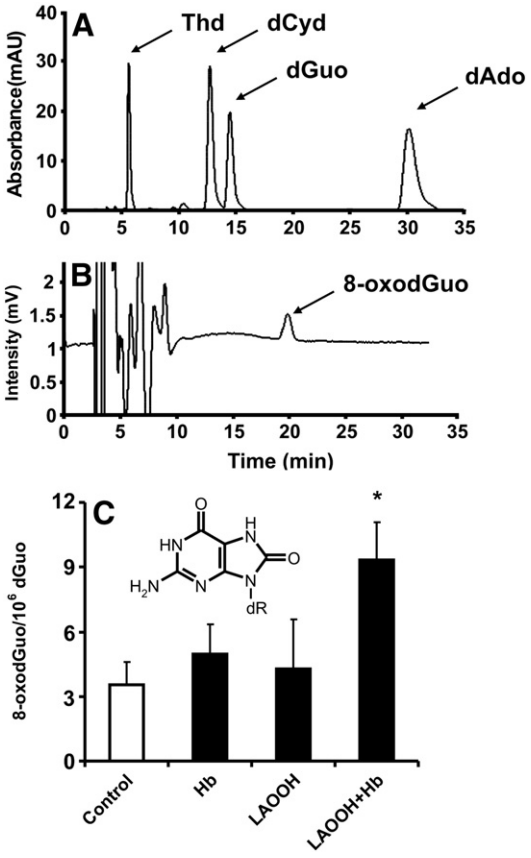

Fig. 6. Evaluation of 8-oxodGuo. For all of the experiments, cells were pretreated with or without 50 μM Hb for 1 h; cells were then challenged with 50 μM LAOOH. Shown is a schematic chromatogram of 100 μg of DNA injected into HPLC/ECD. (A) The UV spectrum (λ = 260 nm) of DNA samples showing thymine (Thd), cytosine (dCyd), guanine (dGuo), and adenine (dAdo). (B) Representation of an electrochemical chromatogram of the same sample with 8-oxodGuo highlighted. (C) The quantification of 8-oxodGuo in treated cells. Per experimental point, three independent experiments were carried out. Bars represent means ± standard deviations. Statistical significance was evaluated by two-way ANOVA (*$p<0.05$). dR, 2-deoxyribose.

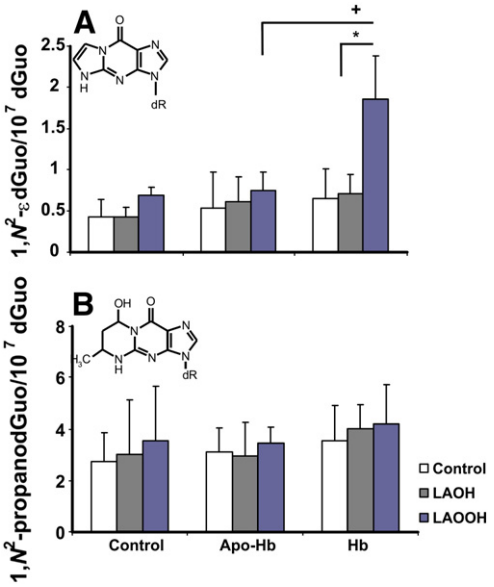

Fig. 7. DNA adduct formation. For all of the experiments, cells were pretreated with 50 μM apo-Hb or Hb for 1 h and, subsequently, challenged with 50 μM LAOOH or LAOH for 1 h. The quantification of (A) 1,N^2-εdGuo and (B) 1,N^2-propanodGuo was carried out as described under Materials and methods. Per experimental point, three independent experiments were carried out. Bars represent means ± standard deviations. Statistical significance was evaluated by two-way ANOVA. +$p<0.05$, statistically different from Hb; *$p<0.05$, statistically different from LAOH.

relevance because such lesions could lead to DNA mispairs, such as the GC/TA transversion. In fact, this kind of transversion is the most commonly found lesion in sporadic colorectal cancer [4], which points, once again, to the relevance of this kind of lesion. Furthermore, a recent study has shown that oxidatively generated DNA damage, measured as 8-oxodGuo formation, correlates with the poor survival of colorectal cancer patients [58].

This work clearly demonstrates that SW480 cells, when pretreated with subtoxic concentrations of Hb, are more sensitive to LAOOH-induced DNA damage. This could be explained by a possible incorporation of the heme group of Hb by SW480 cells. High levels of heme–iron could accelerate the decomposition of LAOOH with the generation of peroxyl and alcoxyl radicals (Eqs. (1) and (2), respectively). These radicals are able to interact with DNA and may result in modifications, such as 8-oxodGuo (Fig. 9, Route I) [59], as follows:

$$\mathrm{LAOOH} + \mathrm{Fe}^{3+} \rightarrow \mathrm{LAOO}^{\bullet} + \mathrm{H}^{+} + \mathrm{Fe}^{2+}, \quad (1)$$

$$\mathrm{LAOOH} + \mathrm{Fe}^{2+} \rightarrow \mathrm{LAO}^{\bullet} + \mathrm{OH}^{-} + \mathrm{Fe}^{3+}. \quad (2)$$

It could be assumed that such species need to be generated near the DNA molecule to interact with it; therefore, one may wonder if such reactions that have been described for model compounds could indeed occur in live cells. A study performed by Ouédraogo et al. [60] showed that the photo-oxidation of membranes led to an increase in lipid peroxidation and DNA strand breaks and that this effect was decreased by the application of Trolox (a hydrophilic antioxidant) and a metal chelator; thus, it was assumed by the authors that radical precursors could be inducing the observed damage, as it was not expected that Trolox would protect against aldehydes generated by the decomposition of LOOH. Furthermore, as it is expected that the lifetime of LAOOH would be increased during oxidative stress, one possible mechanism could involve the sterol carrier protein, SCP-2. It has been shown that this protein was able to strongly inhibit the two-electron reduction of LAOOH by the GSH/GPx1 system [61], which could lead to an increased lifetime of LOOH, thus favoring their intracellular accumulation and their nuclear presence. Although not conclusive, the present results indicate that peroxyl and alcoxyl radicals may indeed be involved in the DNA-damaging effect of LAOOH.

As previously described by our group, lipid peroxyl radicals are able to follow another pathway. Miyamoto et al. [46,62] have shown that linoleic acid hydroperoxides were able to generate singlet molecular oxygen ($^1O_2$) in vitro. In this mechanism, primary or secondary peroxyl radicals ($ROO^{\bullet}$) react by a cyclic mechanism involving a linear tetraoxide intermediate (ROOOOR) that decomposes to generate a ketone (RO), an alcohol (ROH), and molecular oxygen in the excited state. Thus, $^1O_2$ could selectively react with guanine, leading to the formation of 8-oxodGuo [63,64] (Fig. 9, Route II).

Supporting this possible involvement of $^1O_2$ in LAOOH-induced genotoxicity, the incubation of iron and LAOOH with plasmid DNA in D_2O buffer (a known enhancer of $^1O_2$ lifetime) led to an increase in the open circular form of the plasmid in the presence of Fpg, as well as 8-oxodGuo formation (Supplementary Fig. 4). Nevertheless, further investigations are warranted to prove whether such species are indeed formed by LAOOH and could lead to DNA damage in live cells.

Moreover, radicals formed in the cellular membrane are able to attack lipids or decompose to other lipid peroxidation by-products, such as aldehydes, ketones, and epoxides. Such decomposition products are very reactive and could readily interact with DNA to form exocyclic DNA adducts [21,65]. The exposure of cells to Hb and

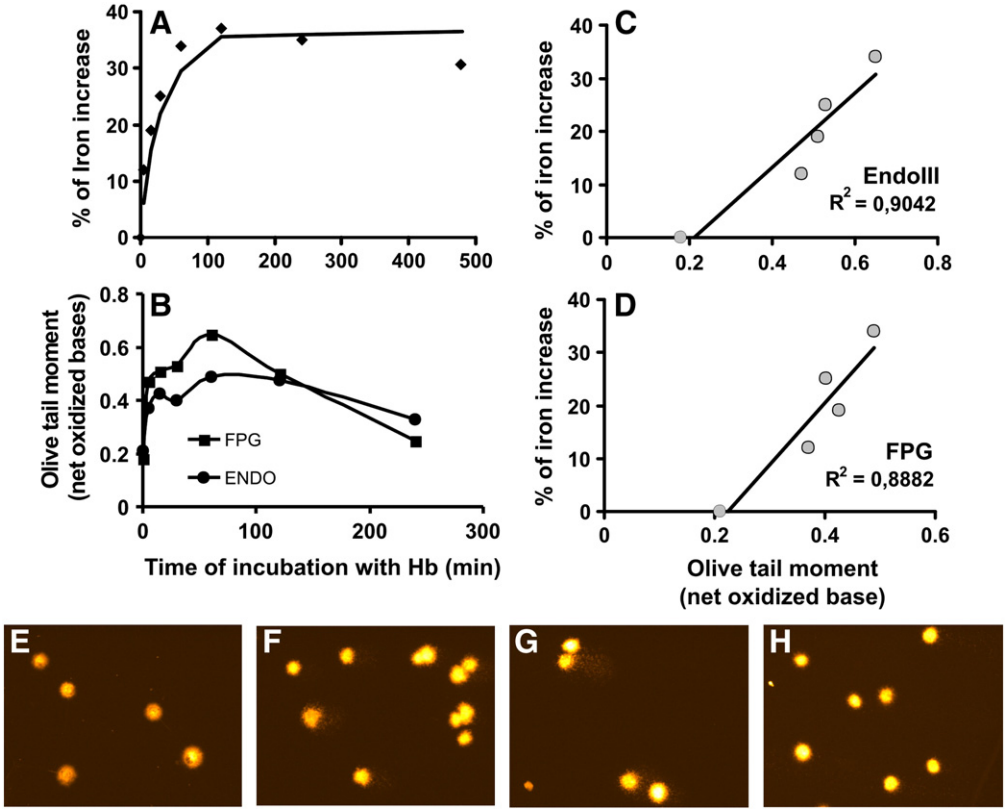

Fig. 8. Iron content and DNA damage. For all of the experiments, cells were pretreated with or without 50 μM Hb for several periods of incubation (0–360 h); cells were then washed and challenged with 50 μM LAOOH. (A) Iron content of cells incubated with 50 μM Hb for various time periods. (B) Evaluation of DNA oxidation measured with the modified version of the comet assay (Fpg and EndoIII digestion). After treatments, the formation of comets was analyzed using a computer-aided analysis system. Per experimental point, three independent experiments were carried out, and, from each culture, 50 cells were analyzed for comet formation. (C and D) Correlation of EndoIII- and Fpg–sensitive sites, respectively, with iron content. (E through H) Representative comet micrographs of cells pretreated with 50 μM Hb for 0, 15, 60, and 240 min, respectively, and then challenged with 50 μM LAOOH.

the further addition of LAOOH generated an increase in 1,N^2-εdGuo. It has been shown that this DNA lesion can arise from the reaction of epoxidized α,β-unsaturated aldehydes with dGuo [21]. Supporting this assumption, the work of Kawai et al. [66] has shown that LAOOH in the presence of metals can decompose to a complex mixture of aldehydes, such as MDA, DDE, and HNE (Fig. 9, Route III, pathway A).

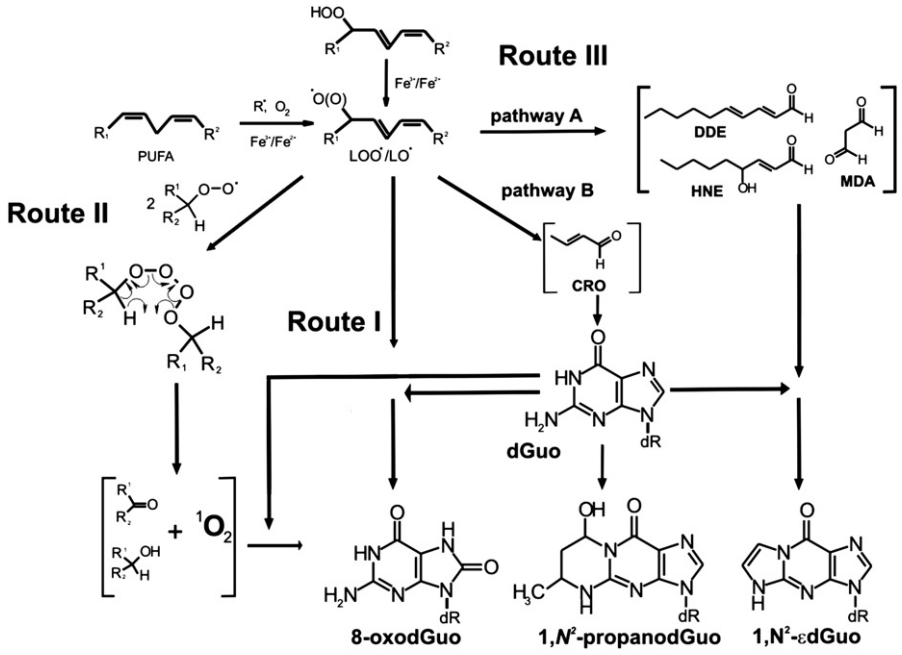

Fig. 9. A schematic representation of the possible mechanisms that account for the Hb/LAOOH-induced DNA damage. dR, 2-deoxyribose.

Such reactions can also produce minor decomposition products, such as crotonaldehyde and acrolein (Fig. 9, Route III, pathway B) [21]. Some of these DNA lesions have been shown to be highly mutagenic and are considered integral in the possible pathways leading to the carcinogenic effects involved in the lipid peroxidation process [67].

In all of the endpoints assayed, we were able to show that a period of preincubation with Hb increased the toxicity of LAOOH and indicated the probable involvement of increased intracellular heme–iron. This was demonstrated by measuring the total iron in lysates of cells exposed to Hb. Heme absorption is mediated by receptor-mediated endocytosis or direct transport [68]. Once absorbed, Fe(II) is then liberated from heme by the action of heme oxygenases [69]. The cellular uptake of inorganic iron is mediated by transport systems, which require the presence of the ferrous Fe(II) ion, which is very unstable and quickly oxidizes to Fe(III). To enable absorption, specialized transmembrane electron transport systems exist, which involve transporters known as ferric-chelate reductases that function by reducing ferric Fe(III) to the ferrous Fe(II) state at the extracellular surface, thus allowing the cell to absorb ferrous iron [70]. To minimize such extracellular processes, we tried to minimize the extracellular presence of Hb by the extensive washing of the cells before adding LAOOH. This was confirmed by measuring the extracellular peroxide consumption, and we were able to show that the extracellular peroxide consumption was the same for every experimental condition, indicating that LAOOH was being consumed inside the cell. Although this approach did not provide subcellular information regarding this oxidative process, it certainly encourages further studies, such as those performed by Kriska et al. [71] using radioactive lipids and measuring their concentration in subcellular fractions. To further address this issue, we also measured the intracellular peroxide content in both the soluble and the lipid fractions after treatment with LAOOH. These experiments indicated that there was an increase in the peroxide content in both compartments; nevertheless, the increase in the lipid fraction was significantly higher. This increase could be expected because, owing to its positive charge, free iron may be attracted by the negatively charged phospholipids (the same could be expanded for the nucleus), thus facilitating lipid peroxidation [72]. Furthermore, the presence of hydroperoxides in the soluble fraction may indeed indicate that this species was translocated and could undergo further decomposition near the nucleus. Regardless, at present, we cannot exclude that the peroxides found in the soluble fraction could have been derived by a chain reaction leading to the generation of other peroxides, such as protein peroxides, which are known to be long-lived [73] and capable of inducing DNA damage [74,75].

To expand upon this observation, we also analyzed the influence of the iron in inducing DNA oxidation with the use of a modified version of the comet assay. In this set of experiments, we showed a strong and positive correlation between the iron content and the DNA fragmentation promoted by LAOOH, which indicated, again, the important role played by heme–iron in LAOOH genotoxicity. It is important to note that we were not able to differentiate whether the intracellular iron found was in the free form, chelated to other biomolecules, or bound to the heme group. We also found that higher exposure times to Hb resulted in a protective effect. This protective effect could be explained by the possible decomposition of the heme group by heme oxygenases to produce CO and bilirubin. Bilirubin has already been reported as a potent lipophilic antioxidant, therefore, it is conceivable that exposure for longer periods to Hb may have increased bilirubin levels, and as a consequence, cells presented an increased protection against the lipid peroxidation induced by LAOOH [76].

We, therefore, could speculate in our model that under basal conditions, oxidative reactions of LAOOH with DNA are favored compared to DNA alkylation. Nevertheless, shifting the iron content to a higher level increased the relative importance of the aldehyde-generated DNA damage, and such species could present a relatively equal effect on DNA modification. Because pretreating cells with Hb and challenging with LAOOH resulted in DNA damage parameters of an approximately threefold (both oxidative and alkylation) increase, one could speculate that under basal conditions, peroxide/aldehyde levels reaching the nucleus are higher compared to a situation involving an elevated iron content. Under such conditions, the peroxide/aldehyde ratio reaching the nucleus may be decreased, and the importance of aldehyde-induced DNA may be relatively increased.

Based on these findings, we propose that high levels of heme–iron lead to an increase in LAOOH-induced genotoxicity, which may be due to the decomposition of LAOOH by heme–iron to generate peroxyl, alcoxyl radicals, $^1O_2$, and aldehydes that could interact with DNA, generating promutagenic DNA lesions.

In conclusion, our results showed that the interaction of Hb and LAOOH at concentrations found in the human diet could produce a synergistic effect on the induction of DNA damage in SW480 cells. These data suggest an increased probability of DNA-damaging events in populations that consume high levels of red meat and fat. Such DNA-damaging events could thus participate in the early stages of cancer development due to an increase in DNA modifications.

Acknowledgments

The authors acknowledge the Brazilian research funding institutions Fundação de Amparo à Pesquisa do Estado de São Paulo, Conselho Nacional para o Desenvolvimento Científico e Tecnológico, Instituto do Milênio: Redoxoma, and INCT de Processos Redox em Biomedicina–Redoxoma and Pró-reitoria de Pesquisa da USP. We thank Professor Frâncisco Laurindo (INCOR) for kindly providing PEG-SOD and PEG-CAT.

Appendix A. Supplementary data

Supplementary data to this article can be found online at doi:10.1016/j.freeradbiomed.2011.04.015.

References

[1] Tomatis, L., Aitio, A., Day, N.E., Heseltine, E., et al. (Eds.), 1990]. Cancer: Causes, Occurrence and Control. IARC Publ., Lyon; 1990.
[2] Cummings, J. H.; Bingham, S. A. Diet and the prevention of cancer. *BMJ* **317:** 1636–1640; 1998.
[3] Stone, W. L.; Papas, A. M. Tocopherols and the etiology of colon cancer. *J. Natl Cancer Inst.* **89:**1006–1014; 1997.
[4] Sjoblom, T.; Jones, S.; Wood, L. D.; Parsons, D. W.; Lin, J.; Barber, T. D.; Mandelker, D.; Leary, R. J.; Ptak, J.; Silliman, N.; Szabo, S.; Buckhaults, P.; Farrell, C.; Meeh, P.; Markowitz, S. D.; Willis, J.; Dawson, D.; Willson, J. K.; Gazdar, A. F.; Hartigan, J.; Wu, L.; Liu, C.; Parmigiani, G.; Park, B. H.; Bachman, K. E.; Papadopoulos, N.; Vogelstein, B.; Kinzler, K. W.; Velculescu, V. E. The consensus coding sequences of human breast and colorectal cancers. *Science* **314:**268–274; 2006.
[5] Ferguson, L. R. Dietary influences on mutagenesis—where is this field going? *Environ. Mol. Mutagen.* **51:**909–918; 2010.
[6] Wynder, E. L.; Kajitani, T.; Ishikawa, S.; Dodo, H.; Takano, A. Environmental factors of cancer of the colon and rectum. II. Japanese epidemiological data. *Cancer* **23:** 1210–1220; 1969.
[7] Bakker, N.; Van't Veer, P.; Zock, P. L. Adipose fatty acids and cancers of the breast, prostate and colon: an ecological study. *Int. J. Cancer* **72:**587–591; 1997.
[8] Howe, G. R.; Aronson, K. J.; Benito, E., et al. The relationship between dietary fat intake and risk of colorectal cancer: evidence from the combined analysis of 13 case–control studies. *Cancer Causes Control* **8:**215–228; 1997.
[9] World Cancer Research Fund Food, Nutrition and the Prevention of Cancer: a Global Perspective. Am. Inst. Cancer Res, Washington, DC; 1997.
[10] Nkondjock, A.; Shatenstein, B.; Maisonneuve, P.; Ghadirian, P. Assessment of risk associated with specific fatty acids and colorectal cancer among French-Canadians in Montreal: a case–control study. *Int. J. Epidemiol.* **32:**200–209; 2003.
[11] Bartsch, H.; Nair, J.; Owen, R. W. Dietary polyunsaturated fatty acids and cancers of the breast and colorectum: emerging evidence for their role as risk modifiers. *Carcinogenesis* **20:**2209–2218; 1999.
[12] Broitman, S. A.; Vitale, J. J.; Vavrousek-Jakuba, E.; Gottlieb, L. S. Polyunsaturated fat, cholesterol and large bowel tumorigenesis. *Cancer* **40:**2455–2463; 1977.

[13] Carroll, K. K.; Khor, H. T. Effects of level and type of dietary fat on incidence of mammary tumors induced in female Sprague–Dawley rats by 7,12-dimethylbenzanthracene. *Lipids* **6:**415–420; 1971.
[14] Prentice, R. L.; Sheppard, L. Dietary fat and cancer: consistency of the epidemiologic data, and disease prevention that may follow from a practical reduction in fat consumption. *Cancer Causes Control* **1:**81–97; 1990.
[15] Sasaki, S.; Horacsek, M.; Kesteloot, H. An ecological study of the relationship between dietary fat intake and breast cancer mortality. *Prev. Med.* **22:**187–202; 1993.
[16] de Kok, T. M.; Zwingman, I.; Moonen, E. J.; Schilderman, P. A.; Rhijnsburger, E.; Haenen, G. R.; Kleinjans, J. C. Analysis of oxidative DNA damage after human dietary supplementation with linoleic acid. *Food Chem. Toxicol.* **41:**351–358; 2003.
[17] Welsch, C. W. Enhancement of mammary tumorigenesis by fat: review of potential mechanisms. *Am. J. Clin. Nutr.* **45:**192–202; 1987.
[18] Ames, B. N. Dietary carcinogens and anticarcinogens: oxygen radicals and degenerative diseases. *Science* **221:**1256–1264; 1983.
[19] Parks, D. A.; Bulkley, G. B.; Granger, D. N. Role of oxygen-derived free radicals in digestive tract diseases. *Surgery* **94:**415–422; 1983.
[20] Blair, I. A. Lipid hydroperoxide-mediated DNA damage. *Exp. Gerontol.* **19:**280–291; 2010.
[21] Medeiros, M. H. G. Exocyclic DNA adducts as biomarkers of lipid oxidation and predictors of disease: challenges in developing sensitive and specific methods for clinical studies. *Chem. Res. Toxicol.* **22:**419–425; 2009.
[22] Esternbauer, H. Cytotoxicity and genotoxicity of lipid oxidation products. *Am. J. Clin. Nutr.* **57:**779–785; 1993.
[23] Bartsch, H.; Nair, J.; Owen, R. W. Dietary polyunsaturated fatty acids and cancer of the breast and colorectum: emerging evidence for their role as risk modifiers. *Carcinogenesis* **12:**2209–2218; 1999.
[24] Reddy, B. S.; Burill, C.; Rigotty, J. Effect of diets high in omega-3 and omega-6 fatty acids on initiation and postinitiation stages of colon carcinogenesis. *Cancer Res.* **51:**487–491; 1991.
[25] Brouwer, I. A.; Katan, M. B.; Zock, P. L. Dietary alpha-linolenic acid is associated with reduced risk of fatal coronary heart disease, but increased prostate cancer risk: a meta-analysis. *J. Nutr.* **134:**919–922; 2004.
[26] Wolff, S. P.; Nourooz-Zadeh, J. Hypothesis: UK consumption of dietary lipid hydroperoxides—a possible contributory factor to atherosclerosis. *Atherosclerosis* **119:**261–263; 1996.
[27] Rohr-Udilova, N. V.; Stolze, K.; Sagmeister, S.; Nohl, H.; Schulte-Hermann, R.; Grasl-Kraupp, B. Lipid hydroperoxides from processed dietary oils enhance growth of hepatocarcinoma cells. *Mol. Nutr. Food Res.* **52:**352–359; 2008.
[28] Kanazawa, K.; Ashida, H. Catabolic fate of dietary trilinoleoylglycerol hydroperoxides in rat gastrointestines. *Biochim. Biophys. Acta* **1393:**336–348; 1998.
[29] Kanazawa, K.; Ashida, H. Dietary hydroperoxides of linoleic acid decompose to aldehydes in stomach before being absorbed into the body. *Biochim. Biophys. Acta* **1393:**349–361; 1998.
[30] Miyamoto, S.; Dupas, C.; Murota, K.; Terao, J. Phospholipid hydroperoxides are detoxified by phospholipase A2 and GSH peroxidase in rat gastric mucosa. *Lipids* **38:**641–649; 2003.
[31] Friedman, E.; Isaksson, P.; Rafter, J.; Marian, B.; Winawer, S.; Newmark, H. Fecal diglycerides as selective endogenous mitogens for premalignant and malignant human colonic epithelial cells. *Cancer Res.* **49:**544–548; 1989.
[32] Jurek, D.; Udilova, N.; Jozkowicz, A.; Nohl, H.; Marian, B.; Schulte-Hermann, R. Dietary lipid hydroperoxides induce expression of vascular endothelial growth factor (VEGF) in human colorectal tumor cells. *FASEB J.* **19:**97–99; 2005.
[33] Norat, T.; Bingham, S.; Ferrari, P.; Slimani, N.; Jenab, M.; Mazuir, M.; Overvad, K.; Olsen, A.; Tjønneland, A.; Clavel, F.; Boutron-Ruault, M. C.; Kesse, E.; Boeing, H.; Bergmann, M. M.; Nieters, A.; Linseisen, J.; Trichopoulou, A.; Trichopoulos, D.; Tountas, Y.; Berrino, F.; Palli, D.; Panico, S.; Tumino, R.; Vineis, P.; Bueno-de-Mesquita, H. B.; Peeters, P. H.; Engeset, D.; Lund, E.; Skeie, G.; Ardanaz, E.; González, C.; Navarro, C.; Quirós, J. R.; Sanchez, M. J.; Berglund, G.; Mattisson, I.; Hallmans, G.; Palmqvist, R.; Day, N. E.; Khaw, K. T.; Key, T. J.; San Joaquin, M.; Hémon, B.; Saracci, R.; Kaaks, R.; Riboli, E. Meat, fish, and colorectal cancer risk: the European prospective investigation into cancer and nutrition. *J. Natl Cancer Inst.* **97:**906–916; 2005.
[34] Lee, D. H.; Anderson, K. E.; Harnack, L. J.; Folsom, A. R.; Jacobs Jr., D. R. Heme iron, zinc, alcohol consumption, and colon cancer: Iowa Women's Health Study. *J. Natl Cancer Inst.* **96:**403–407; 2004.
[35] Tappel, A. Heme of consumed red meat can act as a catalyst of oxidative damage and could initiate colon, breast and prostate cancers, heart disease and other diseases. *Med. Hypotheses* **68:**562–564; 2007.
[36] Sawa, T.; Akaike, T.; Kida, K.; Fukushima, Y.; Takagi, K.; Maeda, H. Lipid peroxyl radicals from oxidized oils and heme-iron: implication of a high-fat diet in colon carcinogenesis. *Cancer Epidemiol. Biomarkers Prev.* **7:**1007–1012; 1998.
[37] Glei, M.; Klenow, S.; Sauer, J.; Wegewitz, U.; Richter, K.; Pool-Zobel, B. L. Hemoglobin and hemin induce DNA damage in human colon tumor cells HT29 clone 19A and in primary human colonocytes. *Mutat. Res.* **594:**162–171; 2006.
[38] Richards, M. P.; Dettmann, M. A.; Grunwald, E. W. Pro-oxidative characteristics of trout hemoglobin and myoglobin: a role for released heme in oxidation of lipids. *J. Agric. Food Chem.* **53:**10231–10238; 2005.
[39] Park, E.; Glei, M.; Knöbel, Y.; Pool-Zobel, B. L. Blood mononucleocytes are sensitive to the DNA damaging effects of iron overload—in vitro and ex vivo results with human and rat cells. *Mutat. Res.* **619:**59–67; 2007.
[40] Knöbel, Y.; Weise, A.; Glei, M.; Sendt, M.; Claussen, W. U.; Pool-Zobel, B. L. Ferric iron is genotoxic in non-transformed and preneoplastic human colon cells. *Food Chem. Toxicol.* **45:**804–811; 2007.
[41] Pierre, A.; Freeman, S.; Tache, M. R.; van der Meer, R.; Corpet, D. E. Beef meat and blood sausage promote the formation of azoxymethane-induced mucin-depleted foci and aberrant crypt foci in rat colons. *J. Nutr.* **134:**2711–2716; 2004.
[42] Lund, E. K.; Wharf, S. G.; Fairweather-Tait, S. J.; Johnson, I. T. Oral ferrous sulfate supplements increase the free radical-generating capacity of feces from healthy volunteers. *Am. J. Clin. Nutr.* **69:**250–255; 1999.
[43] Oates, P. S.; West, A. R. Heme in intestinal epithelial cell turnover, differentiation, detoxification, inflammation, carcinogenesis, absorption and motility. *World J. Gastroenterol.* **12:**4281–4295; 2006.
[44] Pierre, F.; Tache, S.; Petit, C. R.; Van der Meer, R.; Corpet, D. E. Meat and cancer: haemoglobin and haemin in a low-calcium diet promote colorectal carcinogenesis at the aberrant crypt stage in rats. *Carcinogenesis* **24:**1683–1690; 2003.
[45] Govers, M. J.; Termont, D. S.; Lapre, J. A.; Kleibeuker, J. H.; Vonk, R. J.; Van der Meer, R. Calcium in milk products precipitates intestinal fatty acids and secondary bile acids and thus inhibits colonic cytotoxicity in humans. *Cancer Res.* **56:**3270–3275; 1996.
[46] Miyamoto, S.; Martinez, G. R.; Martins, A. P.; Medeiros, M. H. G.; Di Mascio, P. Direct evidence of singlet molecular oxygen $[O_2(^1\Delta_g)]$ production in the reaction of linoleic acid hydroperoxide with peroxynitrite. *J. Am. Chem. Soc.* **125:**4510–4517; 2003.
[47] Wang, H.; Joseph, J. A. Quantifying cellular oxidative stress by dichlorofluorescein assay using microplate reader. *Free Radic. Biol. Med.* **27:**612–616; 1999.
[48] Tatum, V. L.; Ghangchit, C.; Chow, C. K. Measurement of malonaldehyde by high performance liquid chromatography with fluorescence detection. *Lipids* **25:**226–229; 1990.
[49] Dringen, R.; Hamprecht, B. Involvement of glutathione peroxidase and catalase in the disposal of exogenous hydrogen peroxide by cultured astroglial cells. *Brain Res.* **759:**67–75; 1997.
[50] Gay, C. A.; Gebicki, J. M. Measurement of protein and lipid hydroperoxides in biological systems by the ferric-xylenol orange method. *Anal. Biochem.* **315:**29–35; 2003.
[51] Uhl, M.; Helma, C.; Knasmuüller, S. Single-cell gel electrophoresis assay with human-derived hepatoma (HepG2) cells. *Mutat. Res.* **441:**215–224; 1999.
[52] Wang, L.; Hirayasu, K.; Ishizawa, M.; Kobayashi, Y. Purification of genomic DNA from human whole blood by isopropanol-fractionation with concentrated NaI and SDS. *Nucleic Acids Res.* **22:**1774–1775; 1994.
[53] Loureiro, A. P.; Di Mascio, P.; Gomes, O. F.; Medeiros, M. H. G. Trans, trans-2,4-decadienal-induced 1, N(2)-etheno-2′-deoxyguanosine adduct formation. *Chem. Res. Toxicol.* **13:**601–609; 2000.
[54] Garcia, C. C. M.; Freitas, F. P.; Di Mascio, P.; Medeiros, M. H. G. Ultra-sensitive simultaneous quantification of 1, N2-etheno-2′-deoxyguanosine and 1, N2-propano-2′-deoxyguanosine in DNA by on-line liquid chromatography–electrospray tandem mass spectrometry assay. *Chem. Res. Toxicol.* **23:**1245–1255; 2010.
[55] Lipkin, M.; Reddy, B.; Newmark, H.; Lamprecht, S. A. Dietary factors in human colorectal cancer. *Annu. Rev. Nutr.* **19:**545–586; 1999.
[56] Misra, H. P.; Fridovich, I. The generation of superoxide radical during the autoxidation of hemoglobin. *J. Biol. Chem.* **247:**6960–6962; 1972.
[57] Kaneko, T.; Tahara, S. Formation of 8-oxo-2′-deoxyguanosine in the DNA of human diploid fibroblasts by treatment with linoleic acid hydroperoxide and ferric ion. *Lipids* **35:**961–965; 2000.
[58] Sheridan, J. L.; Wang, M.; Tosetto, M.; Sheahan, K.; Hyland, J.; Fennelly, D.; O'Donoghue, D.; Mulcahy, H.; O'Sullivan, J. Nuclear oxidative damage correlates with poor survival in colorectal cancer. *Br. J. Cancer* **100:**381–388; 2009.
[59] Lim, P.; Wuenschell, G. E.; Holland, V.; Lee, D. H.; Pfeifer, G. P.; Rodriguez, H.; Termini, J. Peroxyl radical mediated oxidative DNA base damage: implications for lipid peroxidation induced mutagenesis. *Biochemistry* **43:**15339–15348; 2004.
[60] Ouédraogo, G. D.; Redmond, R. W. Secondary reactive oxygen species extend the range of photosensitization effects in cells: DNA damage produced via initial membrane photosensitization. *Photochem. Photobiol.* **77:**192–203; 2003.
[61] Girotti, A. W. Translocation as a means of disseminating lipid hydroperoxide-induced oxidative damage and effector action. *Free Radic. Biol. Med.* **44:**956–968; 2008.
[62] Miyamoto, S.; Martinez, G. R.; Rettori, D.; Augusto, O.; Medeiros, M. H. G.; Di Mascio, P. Linoleic acid hydroperoxide reacts with hypochlorous acid, generating peroxyl radical intermediates and singlet molecular oxygen. *Proc. Natl Acad. Sci. U. S. A.* **103:**293–298; 2006.
[63] Ravanat, J. L.; Di Mascio, P.; Martinez, G. R.; Medeiros, M. H. G.; Cadet, J. Singlet oxygen induces oxidation of cellular DNA. *J. Biol. Chem.* **275:**40601–40604; 2000.
[64] Ravanat, J. L.; Sauvaigo, S.; Caillat, S.; Martinez, G. R.; Medeiros, M. H. G.; Di Mascio, P.; Favier, A.; Cadet, J. Singlet oxygen-mediated damage to cellular DNA determined by the comet assay associated with DNA repair enzymes. *Biol. Chem.* **385:**17–20; 2004.
[65] Cadet, J.; Di Mascio, P. Peroxides in biological systems. In: Rappoport, Z. (Ed.), The Chemistry of Peroxides, vol. 2. Wiley, New York,pp. 915–999; 2006.
[66] Kawai, Y.; Takeda, S.; Terao, J. Lipidomic analysis for lipid peroxidation-derived aldehydes using gas chromatography–mass spectrometry. *Chem. Res. Toxicol.* **20:**99–107; 2007.
[67] Nair, U.; Bartsch, H.; Nair, J. Lipid peroxidation-induced DNA damage in cancer-prone inflammatory diseases: a review of published adduct types and levels in humans. *Free Radic. Biol. Med.* **43:**1109–1120; 2007.
[68] West, A. R.; Oates, P. S. Mechanisms of heme iron absorption: current questions and controversies. *World J. Gastroenterol.* **14:**4101–4110; 2008.
[69] Raffin, S. B.; Woo, C. H.; Roost, K. T.; Price, D. C.; Schmid, R. Intestinal absorption of hemoglobin iron–heme cleavage by mucosal heme oxygenase. *J. Clin. Invest.* **54:**1344–1352; 1974.
[70] McKie, A. T.; Barrow, D.; Latunde-Dada, G. O.; Rolfs, A.; Sager, G.; Mudaly, E.; Mudaly, M.; Richardson, C.; Barlow, D.; Bromford, A.; Peters, T. J.; Raja, K. B.;

Shirali, S.; Hediger, M. A.; Farzaneh, F.; Simpson, R. J. An iron-regulated ferric reductase associated with the absorption of dietary iron. *Science* **291:**1755–1759; 2001.

[71] Kriska, T.; Levchenko, V. V.; Korytowski, W.; Atshaves, B. P.; Schroeder, F.; Girotti, A. W. Intracellular dissemination of peroxidative stress: internalization, transport, and lethal targeting of a cholesterol hydroperoxide species by sterol carrier protein-2-overexpressing hepatoma cells. *J. Biol. Chem.* **281:**23643–23651; 2006.

[72] Carlsen, C. U.; Moller, J. K. S.; Skibsted, L. H. Heme–iron in lipid oxidation. *Coord. Chem. Rev.* **249:**485–498; 2005.

[73] Wright, A.; Hawkins, C. L.; Davies, M. J. Photo-oxidation of cells generates long-lived intracellular protein peroxides. *Free Radic. Biol. Med.* **34:**637–647; 2003.

[74] Furukawa, A.; Hiraku, Y.; Oikawa, S.; Luxford, C.; Davies, M. J.; Kawanishi, S. Guanine-specific DNA damage induced by gamma-irradiated histone. *Biochem. J.* **388:**813–818; 2005.

[75] Luxford, C.; Dean, R. T.; Davies, M. J. Induction of DNA damage by oxidised amino acids and proteins. *Biogerontology* **3:**95–102; 2002.

[76] MacLean, P. D.; Drake, E. C.; Ross, L.; Barclay, C. Billirubin as an antioxidant in micelles and lipid bilayers: its contribution to the total antioxidant capacity of human blood plasma. *Free Radic. Biol. Med.* **43:**600–609; 2007.